Local network-level integration mediates effects of transcranial Alternating Current Stimulation

Marco Fuscà[1], Philipp Ruhnau[1,2], Toralf Neuling[1,3] and Nathan Weisz[1,3]

1 – Center for Mind/Brain Sciences, University of Trento, Trento, Italy

2 – Department of Neurology, Otto-von-Guericke University, Magdeburg, Germany

3 – Centre for Cognitive Neuroscience, University of Salzburg, Salzburg, Austria

Corresponding Author: Marco Fuscà

Email: marco.fusca@unitn.it

Address: Center for Mind／Brain Sciences

University of Trento

Via Delle Regole 101

38123 Mattarello (TN)

Italy

Abstract

Transcranial alternating current stimulation (tACS) has been proposed as a tool to draw causal inferences on the role of oscillatory activity in cognitive functioning and has the potential to induce long-term changes in cerebral networks. However, effectiveness of tACS underlies high variability and dependencies, which, as previous modeling works have suggested, may be mediated by local and network-level brain states. We used magnetoencephalography (MEG) to record brain activity from 17 healthy participants at rest as they kept their eyes open (EO) or closed (EC) while being stimulated either with sham, weak, or strong alpha-tACS using a montage commonly assumed to target occipital areas. We reconstructed the activity of sources in all stimulation conditions by means of beamforming. The analysis of resting-state brain activity revealed an interaction of the external stimulation with the endogenous alpha power increase from EO to EC. This interaction was localized to the posterior cingulate, a region remote from occipital cortex. This suggests state-dependent (EO vs. EC) long-range effects of tACS. In a follow-up analysis of this online-tACS effect, we find evidence that this state-dependency effect is mediated by functional network changes: connection strength from the precuneus was significantly correlated with the state-dependency effect in the posterior cingulate during tACS. No analogous correlation could be found for alpha power modulations in occipital cortex. Altogether, this is the first strong evidence to illustrate how functional network architectures can shape tACS effects.

Keywords: MEG; tACS; Resting-state; State-dependency; Graph analysis

Introduction

Local and long-range synchronized neural activity reflects coding and transfer of information in the brain, as studies have suggested over the years by *correlating* behavior with oscillatory components of electrophysiological recordings (Cohen & Kohn, 2011). In an attempt to infer more causal relationships between brain oscillations and cognition or behavior, researchers can apply diverse neurostimulation methods that manipulate neural activity. Among the non-invasive brain stimulation methods, transcranial alternating current stimulation (tACS) is gaining remarkable popularity. While online effects of transcranial electrical stimulation on behavior can be investigated, brain signals during stimulation were not recoverable due to the stimulation amplitude, several orders of magnitude higher than neuronal activity. Yet, if the stimulation artifact is consistent and non-saturating, spatial or temporal filtering can recover brain signals even during ongoing stimulation, as some research groups have been showing for the past few years (Soekadar et al., 2013; Helfrich et al., 2014b; see however Noury et al., 2016 and Neuling et al., 2017 for a rebuttal). Neuling et al. (2015) reconstructed brain activity from MEG recordings during simultaneously administered tACS. In this feasibility study, the authors resolved the well-known power increase in posterior alpha activity when closing the eyes (Berger, 1929), showing that oscillatory effects can be recovered at the stimulation frequency. This innovation opens up the possibility to go beyond investigating *offline* aftereffects of the stimulation to understand *online* impact of tACS on brain dynamics.

State-dependency of neurostimulation has been previously established (Neuling et al., 2013; Alagapan et al., 2016). This means that the cortex is more or less susceptible to the externally applied stimulation, depending on its fluctuating patterns of neural activity at local scales as well as on a network-level (for a review see Bikson & Rahman, 2013). State-dependency has broad implications: as the configuration of resting brain networks changes

in many circumstances -most notably when damaged- treatment of neuropsychiatric disorders (Brittain et al., 2013) but also non-clinical applications would benefit considerably from a clearer view of the nature of brain stimulation and its non-linear dependencies. Only a few studies have elucidated the online state-dependency of tACS. For example, a recent study by Alagapan et al. (2016) using modeling, invasive stimulation and ECoG in humans, showed that different behavioral states (such as task-engagement or resting EO / EC) profoundly impact how the same electrical stimulus perturbs ongoing activity. Non-invasively, alpha phase locking with the stimulation signal was shown to change as a function of EO / EC state and current strength (Ruhnau et al., 2016b). No study so far has pursued the issue empirically as to what extent altered network states could mediate tACS effects.

Effects of tACS are seen in brain regions distant from the stimulated cortex but anatomically and functionally connected (Cabral-Calderin et al., 2016). In a framework for explaining prestimulus predispositions on conscious near-threshold perception (Ruhnau et al., 2014), we argue that network-level integration of a neural ensemble determines its propensity to impact downstream regions. In practice, network integration has been operationalized via graph theoretical metrics (Frey et al., 2016), providing support for the framework. Here, we expect that an analogous mechanism could determine how tACS could exert long-range effects. Inter-hemispheric phase synchronization has been shown to be the mechanism behind tACS interference, with functional coupling related to visual perception (Helfrich et al., 2014a). While the latter study shows how tACS affects brain connectivity, we ask the inverted question: how changes in functional network architectures determine the effect of tACS.

In the present study, we analyzed EO and EC resting-state MEG data from Neuling et al. (2015). We expected to see online increases of power at the stimulation frequency that are

dependent on brain state and tACS. In testing the notion that altered functional network architecture could have an influence on tACS effects, we took the most consistent inter-individual state-dependent modulation of network integration (in EO vs. EC, in the precuneus) in the non-stimulated brain and investigated how this relates to the state-dependent alpha power change during tACS. This analysis revealed a significant association, whereas an analogous analysis using power changes during EO and EC in the sham condition was not significant. Overall, our results yield empirical evidence that functional network modulation mediated even by an apparently simple behavioral manipulation can profoundly shape tACS effects.

Materials and methods

Subjects

Seventeen healthy participants (9 males, 28 ± 4 years old; all right-handed) without psychiatric or neurological disorders volunteered for the study. The experiment was approved by the local ethics committee of the University of Trento and carried out in accordance with the Declaration of Helsinki. All participants gave written informed consent prior to its beginning.

Stimuli and procedure

After applying the MEG coils and tACS electrodes to the head and determining the stimulation intensity (see next section), subjects were seated in an upright position in the MEG shielded room. After a brief resting-state measurement block and the estimation of the individual stimulation frequency (see *ISF determination* section below), participants were asked to keep their eyes open (EO) for 2 minutes until a tone and a visual instruction presented on a screen asked them to close their eyes (EC) for another 2 minutes. This was

repeated three times while either no, weak, or strong tACS was applied (see below). The strong stimulation condition was always the last block, to avoid possible aftereffects. For more details on the complete experimental session, see Neuling et al. (2015).

tACS parameters

A battery-operated stimulator system (DC-Stimulator Plus, NeuroConn GmbH, Ilmenau, Germany) was placed outside the magnetically shielded room. It was connected to the stimulation electrodes via the MRI module (NeuroConn GmbH). The stimulator delivered an alternating, sinusoidal current via two conductive- rubber electrodes (NeuroConn GmbH) of 7 by 5 cm applied with a conductive paste (Ten20, D.O. Weaver, Aurora, CO, USA) on the scalp at Cz and Oz of the international 10–20 system, chosen for maximal stimulation intensity in the parieto-occipital cortex (Neuling et al., 2012b). The electrode cables were located on the right side of the participant's head. In order to keep participants naive regarding the stimulation condition, the intensity was kept below the individual sensation and phosphene threshold (for each subject's parameters, cf. Supplementary Table 1 in Neuling et al., 2015). To obtain the threshold, the subject was first familiarized with the skin sensation. Then the subject was stimulated with an intensity of 400 μA (peak- to-peak) at 10 Hz for 5 s. The intensity was increased by steps of 100 μA until the subject indicated skin sensation or phosphene perception or 1500 μA were reached. In the two cases in which the subject already reported an adverse effect at 400 μA, the intensity was reduced to a start level of 100 μA and increased by steps of 100 μA. The individual estimated threshold minus 100 μA was used as stimulation intensity in the strong tACS block. During the sham block, the experimental setup was the same as in the other blocks, but no electrical stimulation was applied. A stimulation intensity of 50 μA was delivered during the weak stimulation.

MEG data recording

Electrophysiological brain activity was recorded at 1000 Hz (on-line band-pass hardware filters: 0.1-330 Hz) using whole head Elekta Neuromag MEG (Elekta Oy, Helsinki, Finland), housed in a magnetically shielded room (AK3b, Vacuumschmelze, Germany). Magnetic brain signal was spatially sampled at 102 positions, each consisting of a channel triplet of one magnetometer and two orthogonal planar gradiometers, yielding 306 sensors overall. Prior to the experiment, fiducials (nasion and left / right periauricular points), the location of five head position indicator (HPI) coils and more than 200 headshape samples were acquired for each participant with a Polhemus Fastrak digitizer (Polhemus, VT, USA). The coils tracked the position of the participants' head during the experiment and the headshape served later for head modeling.

ISF determination

Subjects' alpha frequency, then used as the tACS frequency, was determined by analyzing the initial resting-state block immediately after the measurement (and before the stimulation blocks). The recording was divided into 2-second segments and for each we estimated the power spectra for frequencies ranging from 1 to 25 Hz in .25 Hz steps, after multiplication with a Hanning window and zero-padding of 4 seconds. Clear alpha peaks were identified in the averaged spectral power of the segments and of a chosen group of parieto-occipital gradiometers. In two participants, the peak was not evident from the data, so the frequency analysis was repeated for the EC portion of the first block (no-stimulation condition). The identified alpha peak was then used as the individual stimulation frequency (ISF, referred to as IAF in Neuling et al., 2015) for the tACS.

Offline MEG data analysis

Preprocessing

Continuous data were offline high-pass filtered above 1 Hz and then downsampled to 512 Hz. Then EO and EC resting-state data were segmented into non-overlapping epochs of 2 s aligned to the phase of the stimulation. Epochs in the stimulation-free block were visually inspected to identify noisy, jumpy and dead sensors (then excluded from the whole data).

Source projection of raw data

Sensor space epochs were projected into source space using linearly constrained minimum variance beamformer filters (van Veen et al., 1997), following the procedure for single virtual sensors (www.fieldtriptoolbox.org/tutorial/shared/virtual_sensors) extended to 889 points covering the whole brain. These points were equally spaced by 1.5 cm in Montreal Neurological Institute (MNI) space and warped into individual head-space. The covariance matrix of each single trial was calculated and averaged across epoched data filtered from 1 to 40 Hz and then used to obtain the beamformer filters, together with single-shell head models (Nolte, 2003) derived from the individual head shape and the lead field matrix. Individual trials for each source location was obtained by multiplying the spatial filters with the sensor-level time series.

Beamforming is an adaptive procedure that optimizes spatial filters to restrict covariant signal from surface recordings to a source, localizing and spatially separating activity in the brain. As such, beamformer filters silence sources of noise correlated across sensors and suppress external artifacts in every location (Brookes et al., 2008). In addition to localizing activity in the brain, the aforementioned features seem tailored to reduce the tACS artifact, which is highly correlated noise. No regularization was used to avoid leakage of the tACS artifact to virtual sensors (Neuling et al., 2017). Of the 889 reconstructed sources, only the ones positioned strictly inside the MNI brain were used for subsequent statistical analysis, resulting in 576 virtual sensors. This was done to ensure that no peripheral source capturing

the tACS stimulation was included in the statistics (Neuling et al., 2017). An MNI template brain was used for visualization purposes.

Resting-state power spectrum and PLV

Fourier coefficients were estimated for each epoch of the resting-state data in MEG sensors and in reconstructed activity in brain sources. We used a multitaper spectral estimation (Mitra and Pesaran, 1999) with a fixed smoothing window of ±2 Hz, with a 1 Hz resolution for the frequencies between 1 and 40 Hz and 2 Hz for those between 42 and 84 Hz. The same smoothing parameters for low and high frequencies bands were chosen in order to make comparisons across the entire spectrum.

Mean power densities were determined by averaging the squared absolute value (complex magnitude) of Fourier spectra across epochs and tapers for every sensor and brain source. As a measure of entrainment, we used the inter-trial phase locking value (PLV; Lachaux et al., 1999), calculated as the absolute value of the mean of complex Fourier coefficients. As trials from sensor data were aligned to the phase of the tACS, this gave us an inter-trial coherence to the stimulation at the sources. These averages were computed separately for all stimulation conditions (sham, weak and strong tACS) and for the whole recording with both EO and EC states collapsed together or individually.

Statistical analysis and state-dependency

Power from different conditions was compared using nonparametric cluster-based permutation dependent-samples T-statistics (Maris & Oostenveld, 2007). Cluster randomization was repeated over 5000 permutations. We contrasted relevant conditions at frequencies of interest, alpha and its first 2 harmonics, the first sub-harmonic and 2 control frequencies in between, corresponding to 5, 10, 15, 20, 25 and 30 Hz. Only cluster-corrected p-values lower than $0.008\overline{3}$ (0.05 alpha divided for the 6 frequencies comparisons) were

taken into account. State-dependency (EC vs. EO) of tACS effects was assessed by computing the percent power change of strong tACS relative to sham baseline within subject and condition, as follows:

$$\frac{EC_{strong\ tACS} - EC_{sham}}{EC_{sham}} \ vs \ \frac{EO_{strong\ tACS} - EO_{sham}}{EO_{sham}}$$

The same contrast was repeated for PLV and for the weak tACS condition. Because separate beamforming filters were used, it is not possible to draw a clear interpretation from a direct comparison between different levels of tACS on reconstructed brain sources, but this normalized contrast overcomes this limitation. For illustrative purposes, we also contrasted sham EC versus EO and strong versus sham conditions (both EC and EO).

Graph analysis

We calculated the source-by-source coherence from the Fourier spectra. The absolute value of the imaginary part of coherency was used as the functional connectivity metric to obtain the adjacency matrix. Imaginary coherency guards against spurious correlations due to volume conduction (Nolte et al., 2004). To find the best threshold to binarize the adjacency matrix, we started with the minimum value that ensured, for each frequency, the highest imaginary coherency without disconnected nodes in the graph. This threshold, in which every node in the graph has at least one edge, avoided underestimation of connections. A range of thresholds around this value (±0.1 in steps of 0.02) was then tested to ensure the stability of the effects across choices of threshold. The threshold used was the one that had the highest and most stable effect for nearby values.

Local connectivity for each node was assessed with the following measures: node degree, efficiency, clustering and betweenness (Rubinov & Sporns, 2010). We then applied the same nonparametric cluster-based permutation tests to these measures as we did for power

(also the same frequencies, see *Statistical analysis and state-dependency* section above), contrasting however only EC against EO for sham condition. Via this analysis, we assess the individual propensity of network modulation due to this subtle behavioral change, yielding a stronger argument that potential long-range effects during tACS are mediated by network-level changes. Local efficiency was the only measure that showed a cluster at a p-value lower than $0.008\overline{3}$. This index in particular, as the inverse of the graph average path lengths of all direct connections, reflects the long-range integration of a node in the network. The source with maximum t-value was used as a seed to get individual imaginary coherency values to the source of maximum t-value for the state-dependency contrast. These values were used in the subsequently described seed-based partial correlations.

Regression and partial correlation

We wanted to explore whether the magnitude of the state dependency effect correlated with connectivity. First, we assessed whether the different tACS intensities, with which individual participants were stimulated, would explain some of the variance of the effect (Ruhnau et al., 2016b). Therefore, we extracted for each participant the percent change of the strong tACS normalized EC / EO contrast (see *Statistical analysis and state-dependency* section) from the source with maximum group-level t-value. We regressed the individual tACS intensity with these values. The linear model fit provided the adjusted R-squared and the F statistics.

As we ascertained the relation of stimulation intensity with state-dependency, we had to partial out the variance explained by intensity from subsequent correlations. We were interested in the area with differential network integration profile in EC and EO and its connection with the state-dependency region. We therefore took for each participant the EC / EO percent change of imaginary coherency from the source with maximal significant

difference in local efficiency (see *Graph analysis* section above) to the state-dependency source. We then calculated the Spearman rank partial correlation coefficients between these individual percent changes of seeded imaginary coherency and state-dependency, controlling for tACS intensity. We repeated the partial correlation with percent change of EC / EO power in the occipital cortex instead of seeded coherency, also to control for spurious correlation due to the most variance explained by tACS intensity. Correlation coefficients were t-tested against the two-sided alternative hypothesis of no partial correlation.

Results

Power modulations during tACS

The cluster-based statistic on 10Hz contrasting the strong tACS against sham (calculated with separate leadfield filters) portrayed a strong increase for the stimulation condition distributed in the whole brain, maximally localized in the border between the cuneus and the precuneus (*Figure 1a*). The difference was highly significant ($p_{cluster} < 0.001$), but its interpretation is unclear (see *Discussion*) and it is shown here only for illustrative purposes.

As expected, power at 10 Hz increased in contrasts between EC and EO for all tested frequencies in all stimulation conditions ($p_{cluster} < 0.002$ for sham, *Figure 1b*), but there was no PLV change across all conditions (*Figure S2c*). The largest difference was localized in parieto-occipital areas. Again, this well-established pattern is shown here only to illustrate the topography and its relation with the other effects.

Ongoing brain oscillatory activity interactions of stimulation and brain state was assessed with a stimulation-normalized contrast between EC and EO. No state-dependent power activity was found for this contrast for weak tACS. For strong stimulation, the cluster-based

permutation test revealed a significant difference ($p_{cluster}$ < 0.006) at 10 Hz and the effect was maximally expressed in the posterior cingulate (*Figure 1c*). The largest state-dependent tACS effects in the alpha range were in this region, that is power increases caused by a state change (EC vs. EO) were additionally enhanced by tACS. The effect was only observed for power, and no significant interaction nor change in PLV was found (*Figure S1b* and *S1c)*.

At 30 Hz, the state-dependency contrast revealed a difference in power ($p_{cluster}$ < 0.002), most pronounced in the right superior frontal gyrus (*Figure S1d*). This online cross-frequency modulation related to EO / EC brain state was again driven by power resonance (*Figure S1e*) but not by inter-trial PLV (*Figure S1f*). As in the case of alpha, we cannot assert anything about the sharp increase in frontal 30 Hz power and PLV in strong tACS relative to sham stimulation, because we cannot compare tACS conditions. No other tested frequency showed state-dependent effects.

As these previous analyses established a state-dependent modulation remote to regions showing the primary power change between EC and EO (i.e. posterior cingulate vs. occipital cortex), this implied differences in neural states between these two conditions to mediate this long-range effect. This is the issue pursued in the next sections.

Network-level changes between EC and EO

To expose differences in brain network states between EC and EO, which could potentially influence this novel state-dependent effect, we used graph theoretical analysis of the resting sham data. The whole-brain nonparametric statistic on local efficiency uncovered a cluster in the precuneus for the 10Hz band, which showed a significant increase in EC relative to EO ($p_{cluster}$ < 0.004, *Figure 1d*). Unlike the other frequency bands and the other graph

measures, the effect was stable across a range of values for adjacency matrix thresholding, between 0.12 and 0.26 of absolute imaginary coherency, with a maximum effect at 0.18.

Effects mediating state-dependency

As participants received different tACS strength, we examined the correlation between stimulation intensity and the normalized difference in power denoting state-dependency. We found a correlation between individual intensity and the state-dependent effect (adjusted R^2 = 0.24, p = 0.027; *Figure S3*).

To characterize the relationship of the underlying pattern of connectivity with the state-dependency, the source with maximum statistical value in the efficiency contrast (precuneus, *Figure 1d*) was used as a seed to extract imaginary coherency to the region of the cortex with the state-dependent effect, the posterior cingulate (*Figure 1c*). The partial correlation controlling for tACS intensity revealed that the connection strength between precuneus and posterior cingulate was a predictor of state-dependency (Spearman rho = 0.53, p = 0.036; *Figure 2a*). Still controlling for intensity but using EC / EO alpha power difference as the predicting variable (extracted from the source in the occipital cortex with the strongest contrast; *Figure 1b*) showed no correlation with state-dependency (Spearman rho = -0.25, p = 0.35; *Figure 2b*).

Discussion

State-dependent power effect of tACS

Our analyses uncovered online interactions of tACS with brain states at the alpha frequency. Power enhancements driven by the external stimulation interacted with endogenous alpha increases in the transition from EO to EC. The impact of tACS changed depending on the

brain state: it was more pronounced during EC in the posterior cingulate (*Figure 1c*), an area between the stimulation electrodes but where current flow is not at its peak (*Figure 1a*, but see below). This is further proof for the specificity of tACS efficacy, which is seen in certain tasks, setups and sensory modalities but not in others (Rahman & Bikson, 2013; Veniero et al., 2017). The posterior cingulate cortex was affected differently by the stimulation in different brain states, which raises questions concerning the consequences for resting networks as well as for task-active cognition (Leech et al., 2013).

It is uncertain whether state-dependent effects of tACS in primary target regions (occipito-parietal cortex) are actually absent. Alternatively, it might be that they are simply overshadowed by the dominant Eigenfrequency increase in these regions following closing the eyes (*Figure 1b*, seen also in offline aftereffects in Helfrich et al., 2014b). That is, neural firing rate in occipital and parietal regions might still be influenced by tACS differently in the EC brain state with respect to EO, but if present, this effect is too small relative to the endogenous power modulation.

When contrasting induced alpha power for different tACS conditions, there were differences distributed across the whole brain (*Figure 1a*). This is difficult to interpret, as the variance was probably also driven by the different beamformer filters obtained separately from different conditions. As the filters have to suppress the artifact in the strong tACS condition, their profile is very different from the ones during no stimulation. However, one can appreciate how the cluster reflects maximum current flow of tACS located between the electrodes, as it has been modeled (Neuling et al., 2012b). Even though there is no information on tissue density in our analysis, the effect in source reconstruction shows the current diffusion where the finite-elements model predicts it.

The state-dependent effect of tACS at 30 Hz showed a frontal source distribution and again there was a higher increase in the induced power in the EC state (*Figure S1d-e*). Anatomically connected areas respond, even if not directly stimulated, usually in the range of the natural frequency of their local cortico-thalamic circuit, with frontal regions most sensitive to higher beta (Rosanova et al., 2009). Multiples of the stimulated frequency (harmonics) also have an effect on the brain (Neuling et al., 2017). The cluster in the right frontal pole showing a state-dependent interaction in the second harmonic (30 Hz) seems to be influenced by its preferred frequency. It is hard to declare what drives this modulation, be it EO / EC differential frontal activity (Barry et al., 2007), resting-state network connections from the posterior cingulate, excitability for the natural frequency of the region (Rosanova et al., 2009), or an interaction between these factors during stimulation. Thus, we refrained from investigating this further. Yet again, harmonics and their brain state dependencies are another variable to consider when applying tACS (see also Ruhnau et al., 2016a).

Effects of tACS not driven by phase locking

The interaction of tACS with EC seems to be driven only by power resonance, without a change in PLV (*Figure S1b*). The posterior topography of higher alpha in EC relative to EO, seen in all tACS conditions as clearly as during sham (*Figure 2b*), was likewise not accompanied by phase alignment. This means that a strong continuous entrainment, in which endogenous oscillators align their phase and their frequency to the stimulation, is not seen alongside the power increase or the online state-dependency of tACS. A trend of reduction in synchrony measured by PLV was present in the posterior cingulate but not in the parieto-occipital areas.

As we have seen, the network profile changes in different states, and so could the influence and spread of entrainment in different conditions. Many tACS studies show phasic

modulation of behavior (e.g. Neuling et al., 2012a), which has been attributed to entrainment. State-dependent stimulation-driven phase alignment can be seen after trial averaging (Ruhnau et al., 2016b). Conversely, in another online tACS study, effects on PLV (same formula used in this study) are missing, if not even dampened, at the simulation frequency (Ruhnau et al., 2016a), even though in that paradigm there were several oscillators driven at the same time.

Alternatively, there is some debate on whether entrainment is really the mechanism behind tACS effects (Vossen et al. 2017). Rather than an instantaneous synchronization of endogenous oscillators, tACS has been proposed to be altering synaptic strength, as its mechanism of action to modify brain frequencies (Vossen et al., 2014). Whether inter-trial phase coherence is related to entrainment or not, it is not associated to the increase in source power, especially in this tACS setup (Neuling et al., 2013). If a sub-neural ensemble is entrained, it is not large enough to be the dominant pattern in inter-trial PLV, but there is yet no strong support on the current situation at this level. Effects of tACS related to phase are furthermore not seen in recordings with implanted electrodes (Opitz et al., 2016; Lafon et al., 2017; but see Noury et al., 2017, also for a reproach on phase estimates in deep-brain recordings).

It needs to be clear that tACS in some individual conditions leads to an increase in phase alignment, potentially indicating entrainment (selectively for EO, similarly to Ruhnau et al., 2016b; *Figure S2c*), however since tACS and sham conditions were based on different filters as mentioned above, this needs to be interpreted with caution. Furthermore, our main focus is on the state-dependency of tACS, which doesn't seem to be mitigated by phase alignment in the regions most strongly affected.

Brain connectivity behind state-dependency

Functional connectivity fluctuates continuously, but it varies mostly when the brain changes its *mode* of functioning. This happens during changes between different tasks or in the diverse repertoire of states like vigilance or attention. Even a simple change like closing the eyes creates profound reorganizations of brain activity. In this case, parietal cortices exhibit modifications in their oscillatory balance, especially in the low frequency bands, closely accompanied by changes in connectivity in the same frequencies. In the alpha frequency, the most stable change seems to be the integration of the parietal cortex with the rest of the brain, which increases when eyes are closed (*Figure 1d*). It is reasonable to assume that the variation in connectivity from this region to the rest of the brain is bound to influence other processes that ride on these functional connections (Ruhnau et al., 2014), such as activity modulations caused by tACS.

Reasonably, it appears that tACS influence dependent on the ongoing brain state is mostly driven by the intensity of the electrical stimulation (*Figure S3*). On top of that, regional variation in the system's connectivity are related to the amount of this state-dependency. Namely, the connection strength increase to this region is followed by a better integration and efficiency (*Figure 2a*). Regional alpha power modulations as commonly seen during EC vs. EO, however, do not seem to mediate this state-dependent effect of tACS (*Figure 2b*).

Since functional connectivity indicates electrical information flow among brain areas, it would be evocative to think that it also controls the flow of tACS. The current flow at the neuronal scale should be the same across conditions (*Figure 1a*), yet changes in functional connections during different brain states might guide the impact of tACS distinctively. In other words, connectivity controls and follows patterns of inhibition and excitation in oscillatory activity, so it is likely to interact with tACS. Our data are the first to provide

evidence for this notion, as they reveal tACS-mediated activity in cortical regions distinct from the maximum induced current.

Conclusion

Although there is some convincing evidence on the reliability of tACS and its impact on behavior, its direct influence on brain processes is unknown. The main message of this study is that the online effects of tACS in the parenchyma are also defined by functional factors. Oscillatory activity and connectivity are interwoven, which enables tACS to affect regions that are connected to -but clearly spatially separated from- the focal stimulated zone. As we have seen, a modulation of the functional network architecture by a simple behavioral manipulation has a profound impact on tACS effects. Our analyses confirm that state-dependent tACS efficacy is not due to changes in power but in network reorganization. This finding yields important confirmation that it is connectedness that matters in determining whether activity in a region will affect downstream areas (Ruhnau et al., 2014). As modeling and predicting effects becomes more complex, this should have profound implications for the use of tACS in cognitive and clinical neuroscience, i.e. one should be wary when treating patients based on results obtained in controls.

Researchers need to control as many variables as possible in a neurostimulatory experiment, in which varying a single parameter can reverse its effect (Moliadze et al., 2012; Veniero et al., 2017). Alternate current stimulation is alluring: if it can manipulate physiological frequencies directly, then we can assess whether oscillatory activity actually plays a causal role in cognition and behavior. However, the state-dependency of tACS effects, as well as their nonlinearity, make these current causality assumptions naive and likely inadequate. It is unwarranted to assume a linear mapping between external perturbations and internal brain activity, and neurostimulation paradigms should be

approached with a perspective as informed as possible (for a review see Romei et al., 2016). Thus, it is important to take this into account, both for researchers, applying tasks with distinctive activity and connectivity profiles, and for clinicians, who often have to deal with brain systems that have altered network organizations.

Acknowledgements: This project was supported by the European Research Council (ERC StG 283404). We thank Dr. Elie El Rassi and Dr. Benjamin Timberlake for comments on an earlier version of the manuscript.

Bibliography

Alagapan, S., Schmidt, S. L., Lefebvre, J., Hadar, E., Shin, H. W., & Fröhlich, F. (2016). Modulation of cortical oscillations by low-frequency direct cortical stimulation is state-dependent. *PLoS Biol, 14*(3).

Barry, R. J., Clarke, A. R., Johnstone, S. J., Magee, C. A., & Rushby, J. A. (2007). EEG differences between eyes-closed and eyes-open resting conditions. *Clinical Neurophysiology, 118*(12), 2765-2773.

Berger, H. (1929). Über das Elektrenkephalogramm des Menschen. *Archiv für Psychiatrie und Nervenkrankheiten, 87.*

Bikson, M., & Rahman, A. (2013). Origins of specificity during tDCS: anatomical, activity-selective, and input-bias mechanisms. *Frontiers in human neuroscience, 7, 688.*

Brittain, J. S., Probert-Smith, P., Aziz, T. Z., & Brown, P. (2013). Tremor suppression by rhythmic transcranial current stimulation. *Current Biology*, *23*(5).

Brookes, M. J., Stevenson, C. M., Barnes, G. R., Hillebrand, A., Simpson, M. I., Francis, S. T., & Morris, P. G. (2007). Beamformer reconstruction of correlated sources using a modified source model. *Neuroimage, 34*(4), 1454-1465.

Cabral-Calderin, Y., Williams, K. A., Opitz, A., Dechent, P., & Wilke, M. (2016). Transcranial alternating current stimulation modulates spontaneous low frequency fluctuations as measured with fMRI. *Neuroimage, 141*, 88-107.

Cohen, M. R., & Kohn, A. (2011). Measuring and interpreting neuronal correlations. *Nature neuroscience*, *14*(7).

Frey, J. N., Ruhnau, P., Leske, S., Siegel, M., Braun, C., & Weisz, N. (2016). The tactile window to consciousness is characterized by frequency-specific integration and segregation of the primary somatosensory cortex. *Scientific reports, 6*, 20805.

Helfrich, R. F., Knepper, H., Nolte, G., Strüber, D., Rach, S., Herrmann, C. S., Schneider, R. T., & Engel, A. K. (2014a). Selective modulation of interhemispheric functional connectivity by HD-tACS shapes perception. *PLoS biology*, 12(12), e1002031.

Helfrich, R. F., Schneider, T. R., Rach, S., Trautmann-Lengsfeld, S. A., Engel, A. K., & Herrmann, C. S. (2014b). Entrainment of brain oscillations by transcranial alternating current stimulation. *Current Biology, 24*(3).

Lachaux, J. P., Rodriguez, E., Martinerie, J., & Varela, F. J. (1999). Measuring phase synchrony in brain signals. *Human brain mapping, 8*(4).

Lafon, B., Henin, S., Huang, Y., Friedman, D., Melloni, L., Thesen, T., Doyle, W., Buzsáki, G., Devinsky, O., Parra, L. C., & Liu, A., 2017. Low frequency transcranial electrical stimulation does not entrain sleep rhythms measured by human intracranial recordings. *Nat. Commun. 8*, 1–13.

Leech, R., & Sharp, D. J. (2014). The role of the posterior cingulate cortex in cognition and disease. *Brain, 137*(1).

Maris, E., & Oostenveld, R. (2007). Nonparametric statistical testing of EEG-and MEG-data. *Journal of neuroscience methods, 164*(1).

Mitra, P. P., & Pesaran, B. (1999). Analysis of dynamic brain imaging data. *Biophysical journal, 76*(2), 691-708.

Moliadze V., Atalay D., Antal A., & Paulus W. (2012). Close to threshold transcranial electrical stimulation preferentially activates inhibitory networks before switching to excitation with higher intensities. *Brain Stimul. 5,* 505–511.

Neuling, T., Rach, S., Wagner, S., Wolters, C. H., & Herrmann, C. S. (2012a). Good vibrations: oscillatory phase shapes perception. *Neuroimage*, *63*(2).

Neuling, T., Rach, S., & Herrmann, C. S. (2013). Orchestrating neuronal networks: sustained after-effects of transcranial alternating current stimulation depend upon brain states. *Frontiers in Human Neurosci, 7*.

Neuling, T., Ruhnau, P., Fuscà, M., Demarchi, G., Herrmann, C. S., & Weisz, N. (2015). Friends, not foes: Magnetoencephalography as a tool to uncover brain dynamics during transcranial alternating current stimulation. *NeuroImage*, *118*(C).

Neuling, T., Ruhnau, P., Weisz, N., Herrmann, C. S., & Demarchi, G. (2017). Faith and oscillations recovered: On Analyzing EEG/MEG signals during tACS. *NeuroImage*.

Neuling, T., Wagner, S., Wolters, C. H., Zaehle, T., & Herrmann, C. S. (2012b). Finite-element model predicts current density distribution for clinical applications of tDCS and tACS. *Frontiers in psychiatry, 3.*

Nolte, G., (2003). The magnetic lead field theorem in the quasi-static approximation and its use for magnetoencephalography forward calculation in realistic volume conductors. *Phys. Med. Biol. 48*, 3637–3652.

Nolte, G., Bai, O., Wheaton, L., Mari, Z., Vorbach, S., & Hallett, M. (2004). Identifying true brain interaction from EEG data using the imaginary part of coherency. *Clinical neurophysiology, 115*(10), 2292-2307.

Noury, N., Hipp, J. F., & Siegel, M. (2016). Physiological processes non-linearly affect electrophysiological recordings during transcranial electric stimulation. *NeuroImage*.

Noury, N., & Siegel, M. (2017). Phase properties of transcranial electrical stimulation artifacts in electrophysiological recordings. *NeuroImage*.

Opitz, A., Falchier, A., Yan, C. G., Yeagle, E., Linn, G., Megevand, P., Thielscher, A., Milham, M., Mehta, A., & Schroeder, C. (2016). Spatiotemporal structure of intracranial electric fields induced by transcranial electric stimulation in human and nonhuman primates. *Scientific reports, 6*.

Romei, V., Thut, G., & Silvanto, J. (2016). Information-based approaches of noninvasive transcranial brain stimulation. *Trends in neurosciences, 39*(11), 782-795.

Rosanova M, Casali A, Bellina V, Resta F, Mariotti, M., Massimini, M. (2009). Natural frequencies of human corticothalamic circuits. *J Neurosci, 29.*

Rubinov, M., & Sporns, O. (2010). Complex network measures of brain connectivity: uses and interpretations. *Neuroimage, 52*(3), 1059-1069.

Ruhnau, P., Hauswald, A., & Weisz, N. (2014). Investigating ongoing brain oscillations and their influence on conscious perception – network states and the window to consciousness. *Frontiers in Psychology*, *5*, 1230.

Ruhnau, P., Keitel, C., Lithari, C., Weisz, N., & Neuling, T. (2016a). Flicker-driven responses in visual cortex change during matched-frequency transcranial alternating current stimulation. *Frontiers in human neuroscience, 10*.

Ruhnau, P., Neuling, T., Fuscà, M., Herrmann, C. S., Demarchi, G., & Weisz, N. (2016b). Eyes wide shut: Transcranial alternating current stimulation drives alpha rhythm in a state dependent manner. *Scientific reports, 6*.

Soekadar, S. R., Witkowski, M., Cossio, E. G., Birbaumer, N., Robinson, S. E., & Cohen, L. G. (2013). In vivo assessment of human brain oscillations during application of transcranial electric currents. *Nature communications*, *4*.

Van Veen, B. D., Van Drongelen, W., Yuchtman, M., & Suzuki, A. (1997). Localization of brain electrical activity via linearly constrained minimum variance spatial filtering. *IEEE Transactions on biomedical engineering, 44*(9), 867-880.

Veniero, D., Benwell, C. S., Ahrens, M. M., & Thut, G. (2017). Inconsistent Effects of Parietal α-tACS on Pseudoneglect across Two Experiments: A Failed Internal Replication. *Frontiers in Psychology, 8*, 952.

Vossen, A., Gross, J., & Thut, G. (2014). Alpha power increase after transcranial alternating current stimulation at alpha frequency (α-tACS) reflects plastic changes rather than entrainment. *Brain Stimul, 8*(3).

Figures

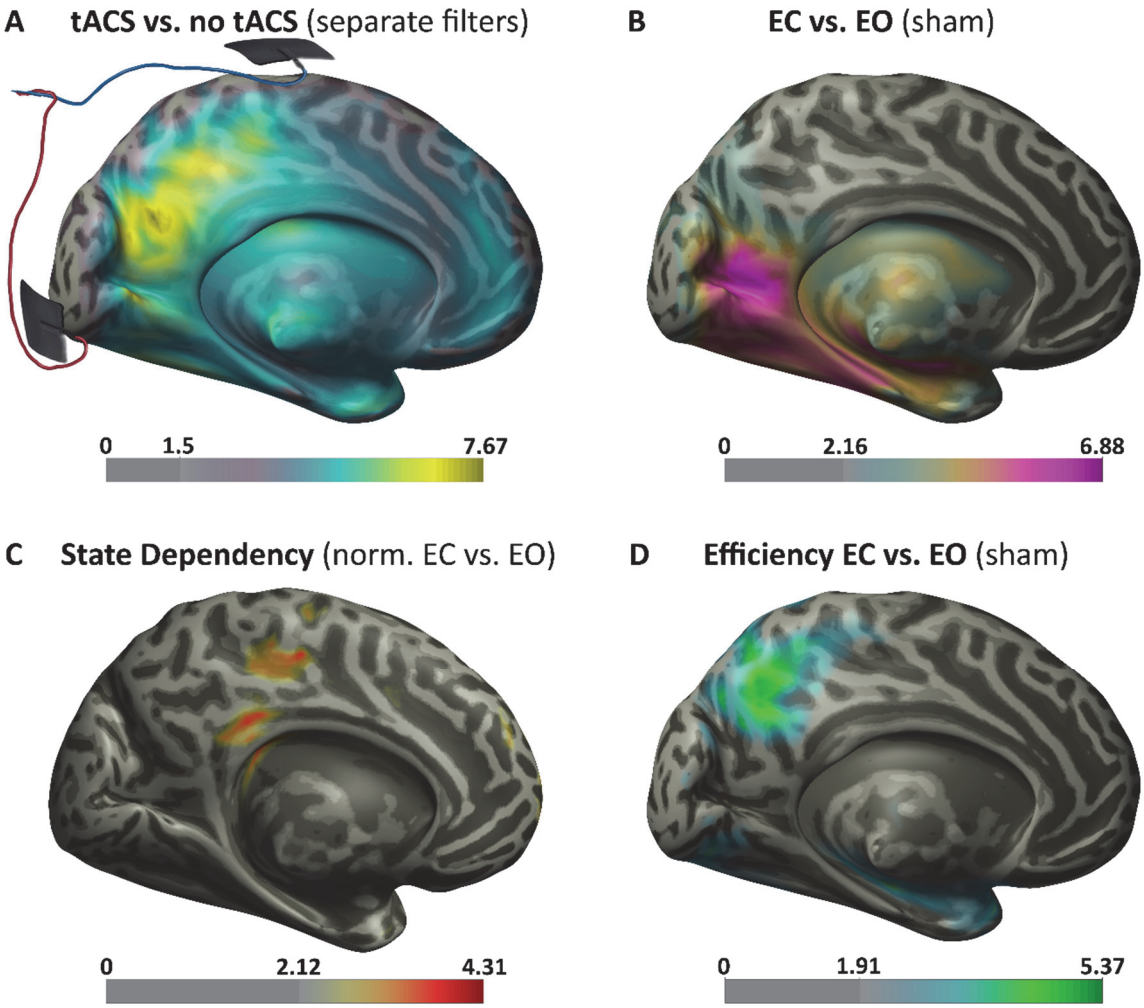

Figure 1. Posterior t-value Topographies
Significant t-values brain maps of the principal effects at 10 Hz during EC or EO and sham or strong alpha tACS. On the bottom of every MNI hemisphere, the color bars with the t-values masked for cluster-corrected $p < 0.05$ significance. Between 0 and the max is the lowest significant t-value. **A.** Medial view of the left hemisphere showing the contrast between strong and sham. Wired rubber patches show the location of the electrodes (attached to the scalp) with which the stimulation was delivered. The strongest effect is located in the medial parieto-occipital cortex, but an interpretation of this contrast is risky (see text). **B.** The well-known increase in alpha power in EC contrasted with EO in occipital and parietal regions. All the tACS conditions showed this difference, but here only the sham contrast is shown. Alpha power differences in this region were used as predictors in the partial correlation of *Figure 2b.* **C.** A stronger alpha increase for EC relative to EO during stimulation in the posterior cingulate, obtained with a normalized contrast denoting state-dependency. The max t-value source was the target of the correlations and seeded coherency of *Figure 2* and *Figure S3*. Unlike the other brains in this figure, here the right hemisphere instead of the left is shown. **D.** Local efficiency increase in EC relative to EO in the precuneus during sham. The source with the strongest contrast was the seed of imaginary coherency used in the partial correlation of *Figure 2a.*

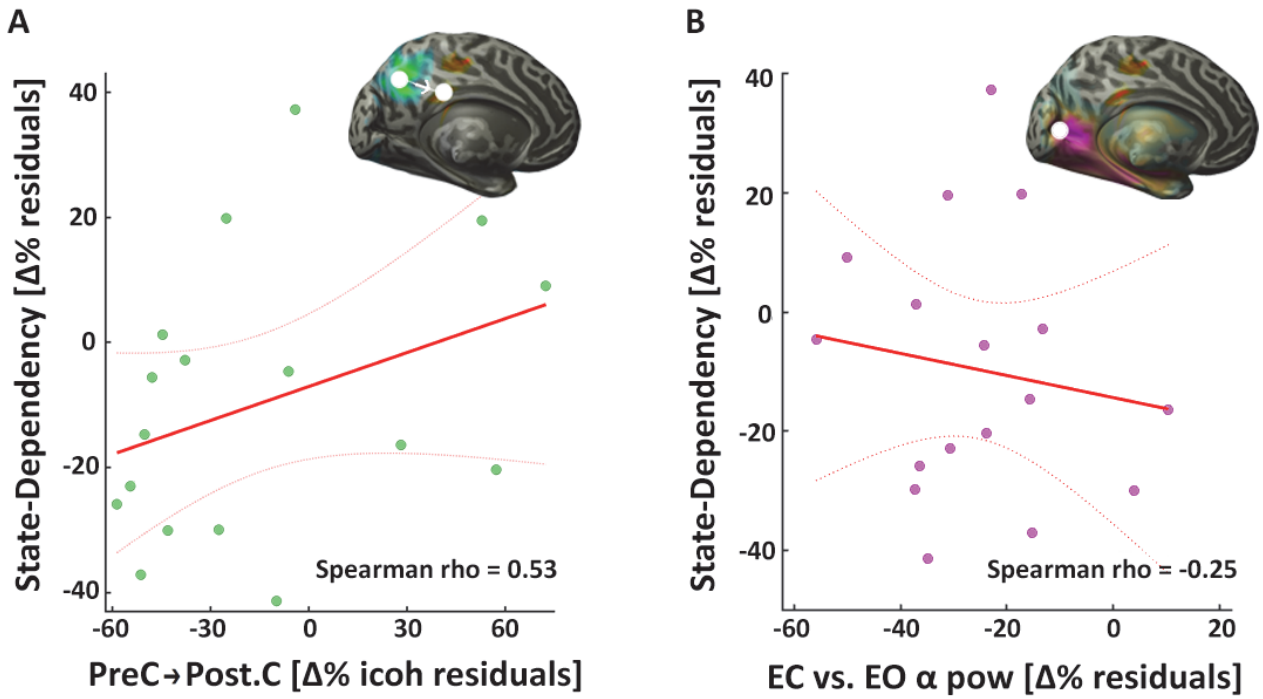

Figure 2. Partial Correlations
Correlations and linear model fits to the individual state-dependency percentage changes. Dotted lines represent the 95% confidence intervals. **A.** Linear model fit of the adjusted values (residuals) of the partial correlation between imaginary coherency (icoh) from the source with maximum local efficiency difference, the precuneus (PreC, MNI coords [-5 -65 40] mm, *Figure 1d*), to the state-dependency one in the posterior cingulate (Post.C, MNI coords [10 -35 25] mm, *Figure 1c*, as the inset on the top right shows). The controlled variable is stimulation intensity, the independent variable in *Figure S1*, here partialed-out. For both the predictor icoh and the predicted state-dependency, these are individual percent change of EC vs. EO. **B.** Same as in *A*, but with alpha power increase in EC vs. EO as a predictor (extracted from the source with maximum t-value, as the inset and as *Figure 1b*). This correlation is non-significant.

Supplementary Figures

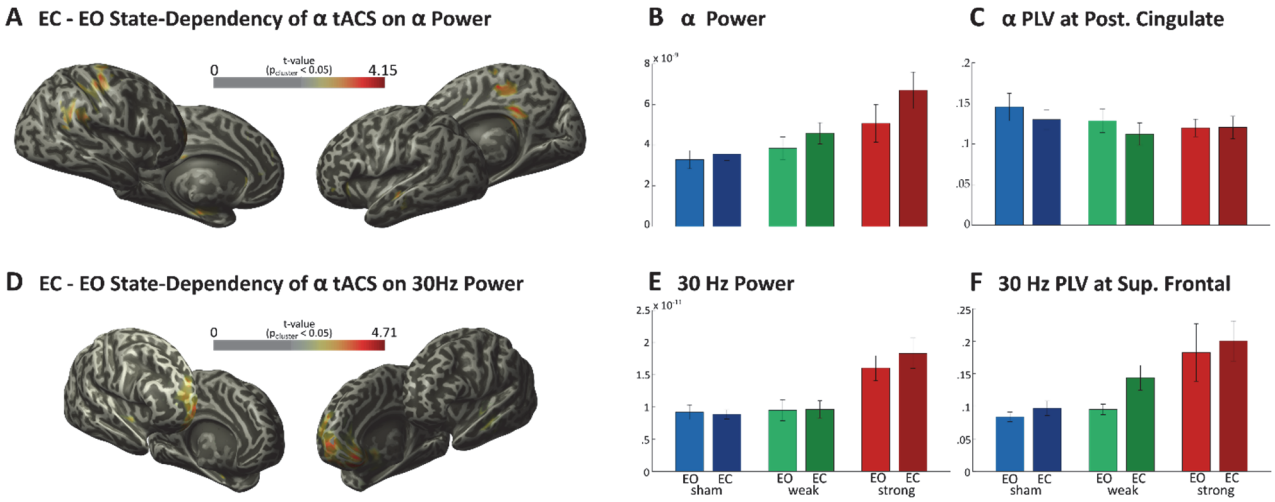

Figure S1. State-Dependent Effects

Strong alpha tACS and EC / EO state interactions at 10 Hz and at 30 Hz. **A.** The projection on the left and right views of the left and right MNI hemispheres (left -medial- view of right hemisphere on the top right is the rotated *Figure 1c*) of the contrast exposing the topography of a stronger alpha increase for EC relative to EO during stimulation in the posterior cingulate. On the top, the color bar with the t-values masked for cluster-corrected p < 0.05 significance. **B.** Alpha Power in the virtual sensor with maximum t-value in the posterior cingulate (MNI coords [10 -35 25] mm, target of the correlations and seeded coherency, *Figure 2*) at different stimulation and EO / EC conditions. The state-dependent effect in power capture by the normalization is discernible from the bigger EO / EC change in strong tACS. **C.** Alpha PLV at the same source. Power increase and the slight PLV decrease visible in the progressive levels of stimulation could be due to filter difference as stated before, so we cannot confidently state anything about that. **D.** Same as in *A*, but the brain is rotated to better show the EO / EC state-dependency at 30 Hz of alpha tACS in the Superior Frontal Gyrus. **E.** Power at 30 Hz in the Superior Frontal Gyrus source (MNI coords [25 70 -5] mm) in all conditions. **F.** PLV at 30Hz at the same position. Bars indicate the condition mean and errorbars the within-subjects 95% confidence intervals.

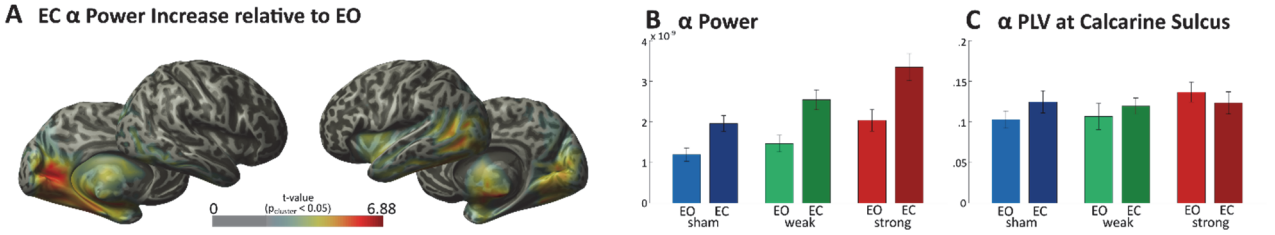

Figure S2. EC Alpha Power Increase

Higher power in EC state relative to EO in occipital regions. **A.** Same as in *Figure S1*, but with the posterior topography of higher alpha power in EC relative to EO (right -medial- view of left hemisphere on the bottom left is the same as *Figure 1b*). **B.** Alpha Power at the Calcarine Sulcus (MNI coords [-5 -95 -5] mm, max t-value, one of the seeds for coherency used in the partial correlations, *Figure 2b*) for the different conditions. **C.** Alpha PLV at the same location. Bars indicate the condition mean and errorbars the within-subjects 95% confidence intervals.

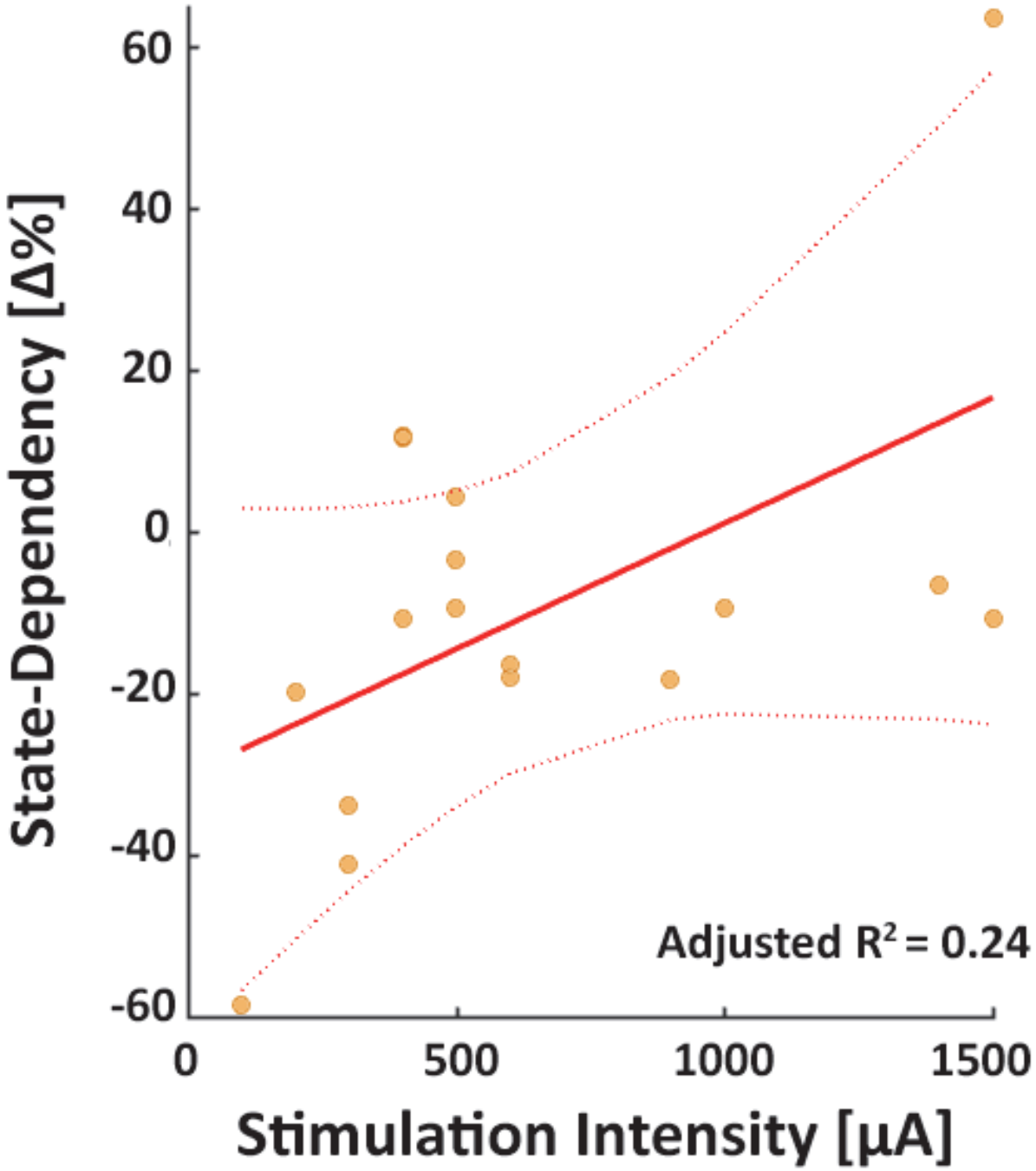

Figure S3. Regression between Intensity and State-Dependency
Correlation between the strong tACS intensity and values for every participant of the normalized change used to detect state-dependency, individual percent change. Dotted lines represent the 95% confidence intervals.